Adsorption of potassium on $Cr_2O_3(0001)$ at ionic and metallic coverages and uv-laser-induced desorption

M. Wilde* and I. Beauport†
Fritz-Haber-Institut der Max-Planck-Gesellschaft, Faradayweg 4-6, D-14195 Berlin, Germany

F. Stuhl
Lehrstuhl für Physikalische Chemie 1, Ruhr-Universität Bochum, Universitätsstrasse 150, D-44780 Bochum, Germany

K. Al-Shamery
Abteilung für Oberflächenchemie und Katalyse, Universität Ulm, Albert-Einstein-Allee 47, D-89081 Ulm, Germany

H.-J. Freund
Fritz-Haber-Institut der Max-Planck-Gesellschaft, Faradayweg 4-6, D-14195 Berlin, Germany
(Received 27 January 1998; revised manuscript received 26 May 1998)

Translational energy distributions of neutral potassium atoms are reported as a function of potassium coverage after uv-laser-induced desorption from well-characterized adsorption sites on an epitaxial film of $Cr_2O_3(0001)/Cr(110)$. Measurements using x-ray photoelectron spectroscopy, low-energy electron diffraction, and work-function measurements revealed that potassium adsorbs in a nonmetallic phase for deposition temperatures around 280–300 K allowing only a maximal saturation coverage to be grown for moderate growth rates. Aggregates are observed after deposition at 90 K; at this temperature any layer thickness is obtainable. The uv-laser-induced desorption for these two different phases was studied using excitation energies of 3.5 eV, 5.0 eV, and 6.4 eV and $(1+1)$-resonantly enhanced multiphonon ionization via the $6p\,^2P$ state for detection. Desorption of potassium atoms from the nonmetallic phase proves to be ten times $[\sigma(6.4\,\mathrm{eV})=(2\pm1)\times10^{-19}\,\mathrm{cm}^2]$ more efficient than desorption from metallic potassium aggregates. The mechanism of desorption from the nonmetallic phase appears to be the inverse harpooning process starting with an ion pair followed by a transfer of hot electrons from the substrate to unoccupied potassium states to neutralize the initially positively charged potassium. The maximum of the translational energy distribution (starting at 0.65 eV for low coverages) decreases with increasing potassium coverage and is by a factor of approximately 4 smaller for desorption from large potassium aggregates (0.16 eV). The decrease of the translational energy with increasing coverages for isolated atoms is ascribed to an increasing lateral interaction between the adsorbates and a concomittant smooth change of the ionicity of the atoms from partially ionic to neutral. [S0163-1829(99)01619-7]

I. INTRODUCTION

The understanding of the photochemistry of adsorbates on single-crystal surfaces has largely improved in the past years (Refs. 1–5, and references therein). While the knowledge on weakly bound systems is quite elaborate, the knowledge on strongly bound systems such as laser-induced metal-atom desorption is still controversial.

Popular model systems are alkali aggregates adsorbed on a variety of surfaces like caesium adsorbed on Cu(111),[6] sodium adsorbed on germanium,[7] or insulating surfaces like lithium fluoride,[8–13] sapphire,[14] and mica,[13,15] as well as coalesced sodium droplets and thin continuous films[16–20] and potassium adsorbed on LiF(100) (Ref. 12) and graphite[21–23] (see also the review by Madey *et al.*, which includes data on electron stimulated and thermal desorption[24]).

The general belief is that desorption is initiated by a plasmon excitation within the aggregates or films for the wavelengths used. The latter were below the band gaps of the supports in all cases. However, quite different experimental results on translational energy distributions of desorbing sodium have led to different desorption models. Hoheisel and co-workers[8–12] and Bonch-Bruevich and co-workers[17–20] explain their data by a transfer of the initial collective electron oscillation to localized single electron excitation followed by a preferential desorption from edge or defect sites. Rubahn and co-workers suggest a scattering of the initial surface plasmon of sodium with surface vibrations to cause desorption to explain their rather deviating results on translational energy distributions.[13,15]

Interesting in this context are results obtained by Hellsing and co-workers[21,22] and Chakarov *et al.*[23] on the system of potassium on graphite. They found a preferential desorption from the ionic two-dimensional (2D) phase of potassium on graphite while a metallic adsorbate state was not photoactive when using a mercury lamp for desorption. The mechanism they discuss is an inverse harpooning mechanism in which hot electrons from the substrate are transferred back to an unoccupied potassium level.[21–23]

The results on graphite raise the question of which role aggregate edges in contact with the support and the interaction between potassium and the support in general may play in the desorption process. Little is known on this subject except for graphite. We were therefore interested in a system

for which both photodesorption from ionic species as well as from a metallic phase can be observed to bridge the gap between the different data. On oxide surfaces a gradual change of alkali atoms from ionic to metallic species with increasing coverage is not unusual.[25] A suitable system is potassium adsorbed on $Cr_2O_3(0001)$ exhibiting an interesting variety of phases depending on the growth conditions. The data presented in this paper are a substantial extension of a first publication that was restricted to some results on the laser desorption from the nonmetallic disperse phase.[26]

In contrast to metal substrates adsorption of alkali and alkali-earth metals on insulators like oxide surfaces are not always explained by a simple charge transfer to the substrate but can be more complex than on metals. Not only alloy formation can occur but also redox reactions as well as mixed oxide formation is possible. A redox reaction can be a full or partial reduction of the substrate metal ions and a related oxidation of the alkali metal followed by oxide formation. Such an alkali oxide formation can induce substantial changes within the surface structure.[27,28] It is therefore essential to, first of all, understand the way alkali atoms interact with the surface before addressing the problem of their photochemistry.

This paper is therefore divided into two subsections. The first section deals with the characterization of the growth mode of potassium on the $Cr_2O_3(0001)$ surface at room temperature and at liquid-nitrogen temperature as studied with XPS (x-ray photoelectron spectroscopy), LEED (low-energy electron diffraction), and work-function measurements. While only a saturation coverage of a nonmetallic species was obtained at room temperature for moderate deposition rates any layer thickness of metallic potassium was grown at 90 K. This behavior is due to the absence or presence of nucleation centers for further growth in the form of small aggregates and a different mobility of the atoms on the surface.

In the second section the laser-induced desorption of neutral potassium atoms will be reported using a $(1+1)$-REMPI (resonantly enhanced multiphoton ionization) detection scheme. We shall show that the laser-induced desorption, particularly the translational energy distributions are strongly influenced by the lateral interatomic interaction when changing from single ionic to neutral species to metal aggregates.

II. EXPERIMENTAL SETUP

A. General setup

The experiments were carried out in a UHV system described elsewhere.[29] The apparatus was equipped with LEED, AES (Auger electron spectroscopy), XPS, XAES (x-ray Auger electron spectroscopy), and a TDS facility (thermal desorption spectroscopy). $Cr_2O_3(0001)$ was grown as an epitaxial film on a Cr(110) single crystal cleaned prior to oxidation via prolonged sputter-annealing cycles with neon ions. A well-ordered oxide film of 4–5 nm thickness was obtained after oxidizing the metal surface in an atmosphere of 10^{-6} Torr of oxygen at 500 K and annealing to 1000 K. The oxide film was freshly prepared by a sputtering-annealing-oxidation cycle prior to each photodesorption measurement instead of cleaning the oxide film through thermal desorption of potassium. Since potassium may diffuse through the oxide film, this procedure avoids potassium contamination of the Cr(110) crystal and related uncontrollable segregation of potassium on the oxide film in later experiments. The sample was connected by tungsten wires to a sapphire block attached to a copper liquid-nitrogen reservoir. Heating was performed via electron bombardment. Temperature control was performed with a thermocouple (chromel-alumel) spot welded to the crystal side. Deposition of potassium was performed at two different surface temperatures, 90 K and 300 K, from a thoroughly outgased standard SAES getter. The chamber pressure did not exceed $3-8\times10^{-10}$ Torr during deposition. Routinely, the surface cleanness was checked by XPS.

Potassium was desorbed by irradiating the surface with a broadband excimer laser (Lambda Physik EMG 200) run at three photon energies (3.5 eV, 5.0 eV, and 6.4 eV) with pulse lengths of 15 ns and laser fluences of typically 1 mJ/cm^2 directed normal to the surface. Desorbing potassium atoms were detected using $(1+1)$-REMPI in the gas phase with the laser beam running parallel to the surface at a distance of 32 mm. We used a tunable excimer laser (XeCl, Lambda Physik LPX 205 i cc) pumped dye laser (Lambda Physik LPL 3002) with a bandwidth of 0.0015 nm, and pulse energies of 6–10 mJ. Wavelengths between 344 nm and 345 nm were generated using *p*-terphenyl dye dissolved in dioxane. The ions generated in the REMPI process were deflected perpendicular to the desorption and detection laser beam direction by a repeller electrode and collected in a detector consisting of a flight tube, microchannel plates, and a phosphor screen. Time-of-flight spectra were obtained from a systematic variation of the time delay between the detection and desorption laser pulses. For this purpose the wavelength of the detection laser was fixed to the maximum of one of the two REMPI transitions of potassium. The velocity of the desorbing atoms was calculated from the delay times and the known flight distance of the atoms at the detection laser beam.

B. REMPI detection scheme for potassium

For the detection of desorbing potassium atoms we used a $(1+1)$-REMPI detection scheme involving the transitions $6p\,^2P_{1/2,3/2}\leftarrow 4s\,^2S_{1/2}$ at $\lambda^{air}=344.637$ nm and $\lambda^{air}=344.738$ nm corresponding to 28 999.27 cm^{-1} and 29 007.71 cm^{-1}, respectively.[30,31] By absorption of a second photon from the same linearly polarized laser pulse, the intermediate $6p\,^2P_{1/2,3/2}$ states are ionized. The ionization energy of gas phase potassium atoms is 35 009.77 cm^{-1} (4.341 eV, $\lambda=285.635$ nm).[30] The spectrum obtained by tuning across the two absorptions is shown in Fig. 1. The ratio of the integrated line intensities was approximately two as expected from the $^2P_{1/2}$ and $^2P_{3/2}$ degeneracies. The intensities were found to increase linearly with the laser intensity. The detection limit was estimated to be roughly 10^5 atoms/cm^3. This even conservative estimate was based on the desorption signal of a known potassium coverage (determined with XPS) for which the desorption cross section and the angular distribution obtained from a Doppler-profile analysis were known. This high sensitivity allowed to detect desorption easily from coverages as low as $10^{-5}-10^{-4}$ of a monolayer.

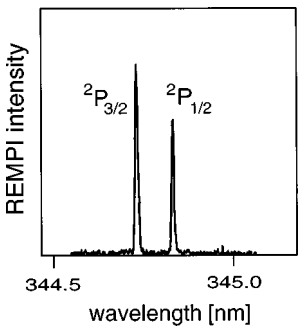

FIG. 1. $(1+1)$-REMPI spectrum of potassium desorbing from the $Cr_2O_3(0001)$ surface including transitions from the $4s\ ^2S_{1/2}$ to the $6p\ ^2P_{1/2}$ and the $6p\ ^2P_{3/2}$ intermediate states.

III. RESULTS AND DISCUSSION

A. Characterization of the adsorption of potassium on $Cr_2O_3(0001)$

1. LEED measurements

No LEED superstructure was observed in any of the preparations. The substrate spots of the $Cr_2O_3(0001)$-LEED pattern became increasingly diffuse at higher coverages. This indicates that potassium grows in a disordered way to form a (1×1) superstructure at a monolayer coverage. However, in some cases alkali concentrations have to be accurate by 1% of a monolayer for ring structures to appear after alkali adsorption so that our observation does not necessarily exclude the existence of any superstructure.[32]

2. XPS: The nonmetallic phase

Figure 2(a) shows XP spectra of the K $2p$ emission of an adsorbate on the $Cr_2O_3(0001)$ surface prepared at room temperature as a function of different potassium coverages using a low deposition rate. The highest coverage shown in the figure corresponds to the saturation coverage, which could not be surpassed even with excessive dosing at room temperature. Potassium coverages are given in relative numbers as multiples of this saturation coverage obtained from integrating the K $2p$ spectra. Absolute values were not obtained because of the lack of information on LEED superstructures.

The splitting of the K $2p$ signal is due to the 3/2 and 1/2 doublet resulting from the spin-orbit coupling of the core-hole states in the $2p$ level. The intensity distributions can well be reproduced by two Voigt profiles with maxima at 294.2 eV ($2p_{3/2}$) and 296.9 eV ($2p_{1/2}$) with a ratio of the integrals of 2:1 reflecting the degeneracy of the two states of 4:2. The simulations are shown as gray areas underneath the measured curve. In the literature a value of the K $2p$ emission of metallic potassium of 294.4 eV ($2p_{3/2}$) and 297.2 eV ($2p_{1/2}$) is reported.[33] On the other hand, an average shift of about 1.5 eV towards lower binding energies is found for ionic potassium. Values of 292.9 eV ($2p_{3/2}$) and 295.67 eV ($2p_{1/2}$) have been observed for KCl.[33] The values obtained for the $K/Cr_2O_3(0001)$ system are shifted by only about 0.2–0.3 eV with respect to the values of metallic potassium. However, the K $2p$ spectrum of metallic potassium typically shows additional features due to plasmon excitations (as will also be seen further below). *A priori* formation of metal aggregates and not fully be ruled out as XPS is not a very sensitive method for detecting plasmon excitation. In fact, such extra features can be observed at room temperature at coverages close to the saturation coverage for high deposition rates [Fig. 2(b), upper trace]. These films are metastable as the plasmonic features immediately disappear after an increase of the surface temperature to 450 K [Fig. 2(b), lower trace]. The reason for aggregate formation at high deposition rates might be either that the potassium getter emits clusters for those rates or the deposition rate is large enough to surpass a critical value for formation of nucleation centers to occur.[25] Nucleation centers exceeding a critical size might be necessary to stabilize the metallic aggregates at room temperature. Increasing the mobility of potassium atoms by an increase of the temperature for such a coverage is sufficient to destroy the aggregates. This would imply a repulsive interaction between potassium atoms and a high mobility of single potassium atoms on the surface allowing to take energetically favorable positions after hitting the surface at 280–300 K.

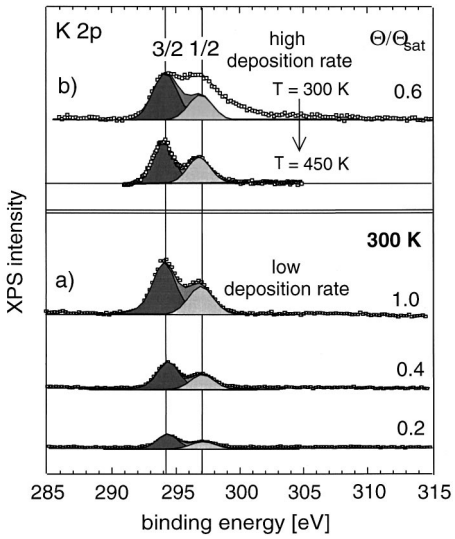

FIG. 2. Dispersive potassium phase on $Cr_2O_3(0001)$: (a) Dotted curve: XP spectra of the K $2p$ emission as a function of increasing potassium coverage deposited with a low deposition rate at room temperature on $Cr_2O_3(0001)$; gray curves: fits assuming two Voigt profiles with maxima of $2p_{3/2}$ and $2p_{1/2}$ (ratio of the integrals of 2:1 reflecting the multiplicity of the two states of 4:2); coverages given as multiples of a maximal saturation coverage θ_{sat} at room temperature obtained from the integrals of K $2p$ XP spectra; detection geometry: 30° off normal emission. (b) Upper curve: like (a) but dosing with a high deposition rate; lower curve: spectrum of upper curve after short flash to 450 K.

The K $2p$ spectrum indicates that the amount of charge transferred to the substrate is only small, which is also reflected in the XP spectra of the substrate. Different to reactive systems such as Mg on $Cr_2O_3(0001)$ (Ref. 28) no changes within the XP spectra of the Cr $2p$ and O $1s$ emission are observed for potassium adsorption except for a shift towards higher binding energies of up to 0.4 eV due to band-bending effects. As shown in Fig. 3, the integral intensity of the Cr $2p$ emission becomes less intense with potassium adsorption, while the O $2p$ emission remains constant indicating a preferential interaction of the potassium atoms with the chromium ions. A decrease of the O $1s$ signal starts notice-

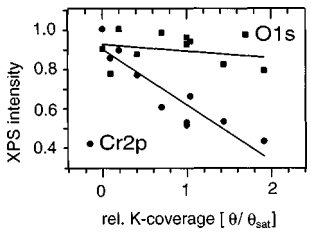

FIG. 3. Dispersive potassium phase on $Cr_2O_3(0001)$: XPS intensity of the Cr $2p$ (dots) and O $1s$ (squares) as a function of potassium coverage are given as multiples of a maximal saturation coverage θ_{sat} at room temperature obtained from the integrals of K $2p$ XP spectra.

ably for depositions at 90 K at coverages larger than the corresponding saturation coverage at room temperature (Fig. 3).

3. Work-function measurements

To obtain more quantitative information on the charge-transfer, work-function measurements have been performed by monitoring the low-energy cutoff of the photoelectron spectra. The work-function curve of Fig. 4 was obtained by successively increasing the amount of potassium at 300 K. After each step the amount of deposited potassium was controlled via XPS measurements and is given in Fig. 4 as multiples of the saturation coverage. After reaching the saturation coverage the sample was cooled to 90 K, and the deposition was continued. The work-function change was not corrected for band-bending effects as the exact course of the rather small band bending at low coverages was not resolved within our experiments. The work function for the clean $Cr_2O_3(0001)$ was found to be 4.8 ± 0.2 eV in agreement with previous results.[28,34,35] The error bars reflect the uncertainty of evaluating the work-function change with XPS. With increasing potassium coverage a mainly linear decrease of the work function is observed until reaching a shallow minimum at 2.0 eV for half the saturation coverage. For thicker layers ($\Theta > \Theta_{sat}$) at 90 K the work function approaches the value of pure potassium metal of 2.1 eV, which is well within the range of 2.0–2.3 eV reported from other groups.[36,37] The minimum in the work-function curve appears only for the deposition procedure described above. However, the experimental error bars of the single measurements are larger than the depth of the minimum itself, and one might argue whether the minimum exists at all.

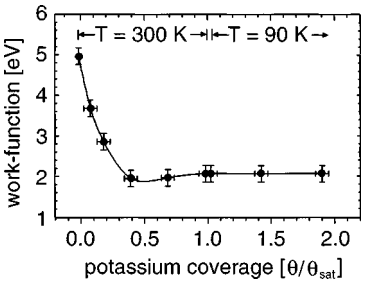

FIG. 4. Work-function change (measured at the low-energy cutoff of the XP spectra) as a function of potassium coverage on $Cr_2O_3(0001)$; coverages are given as multiples of a maximal saturation coverage θ_{sat} at room temperature obtained from the integrals of K $2p$ XP spectra.

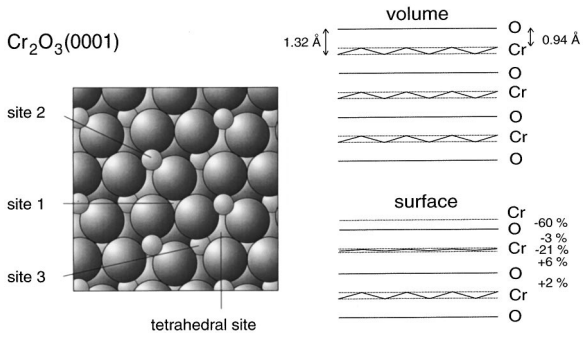

FIG. 5. Left: schematic drawing of the top view of the structure of the $Cr_2O_3(0001)$ surface terminated by half a layer of chromium ions; right: schematic drawing of the side view of the stacking of chromium and oxygen layers of Cr_2O_3 along the (0001) direction for the bulk (upper drawing) and the depolarized surface (lower drawing) (data from Ref. 43). Small circles: chromium ions; large circles: oxygen ions.

4. The structure of the nonmetallic phase

The work-function curve of the system $K/Cr_2O_3(0001)$ shows the classical behavior as found for many alkaline adsorbates on metal surfaces,[38] which can be described by the Langmuir-Gurney model at low coverages.[39–41] This model attributes the linear decrease of the work function to the formation of a dipole layer after charge transfer of the *s*-valence electrons to the substrate. At higher coverages the work function increases after running through a minimum because lateral interactions between the dipoles act as a depolarization field. At high coverages the work function of the pure alkali metal is reached. However, it has been observed that the depolarization on oxidic surfaces is not necessarily as strong as on metal surfaces.[25] In a number of cases for alkali adsorption on oxide surfaces, a missing minimum of the work-function change is not unusual reflecting the rather gradual change from ionic to metallic species.[25]

Assuming a saturation coverage with one potassium atom per unit cell of $Cr_2O_3(0001)$ equivalent to a density of 4.6×10^{14} atoms per cm^2 for a monolayer[35] the dipole moment μ of the potassium atoms can be estimated from the linear part of the decreasing work-function curve φ according to

$$\Delta\varphi = \mu(\theta)\,\theta\sigma_{ML}/\varepsilon_0 \qquad (1)$$

with $\Delta\varphi$ being the work-function change, θ being the coverage, σ_{ML} being the monolayer density, and ε_0 being the permittivity constant ($=2.655\times10^{14}\,D\,V^{-1}\,cm^{-2}$).[42] As the work function drops linearly from 4.8 eV for the clean $Cr_2O_3(0001)$ surface to 2.8 eV at $0.2\theta_{sat}$, a dipole moment of 5.77 D (1.925×10^{-29} Cm) is obtained. In order to estimate the related charge transfer we have to (1) consider the oxide surface structure and (2) speculate about the adsorption position of the potassium and related bond lengths.

(1) Chromium oxide is a corundum-type oxide. The stacking of layers along a direction perpendicular to the (0001) plane in the bulk consists of basically flat oxygen layers alternating with buckled metal ion layers as shown schematically in Fig. 5. An electrostatically stable (0001) surface is

obtained by cutting the stack of layers within the buckled metal ion layer.[43] This halves the number of metal ions left on the surface and stabilizes the polar surface. Further, strong relaxation of the first four layers leads to surface energies close to those found for nonpolar oxide surfaces with nondivergent surface potentials as shown in Fig. 5.

(2) Potassium mainly interacts with the chromium ions. The most plausible adsorption sites are site 1 or site 3. On these sites the positive charge of the potassium adsorbate can be stabilized by the threefold hollow position on the negatively charged oxygen atoms in accordance with findings on other oxidic surfaces.[25] In recent *ab initio* calculations on the relaxed chromium oxide surface, Leitheuser and Staemmler found that the preferential adsorption site of an alkali atom modeled by a positive point charge is rather site 1 than site 3.[44] In their calculations the charge of the chromium ion is reduced to $+2$ to account for the charge transfer. This situation resembles that of potassium cations in K_2O with potassium being tetrahedrally surrounded by the oxygen ions within the bulk. The distance of the potassium to the plane of the three oxygen atoms in K_2O is 0.93 Å.[45] The experimentally found distance between the oxygen layer and the lower half of the buckled chromium layer of the relaxed $Cr_2O_3(0001)$ surface is 1.21 Å.[43]

Assuming the distances mentioned above, the partial charge transfer can roughly be estimated to be 56% of an elementary charge ($1.602\,10\times10^{-19}$ C) according to the Helmholtz equation $\mu = ql$ (q being the partial charge and l being the distance from the center of mass of the K atom to the chromium ion).[37] For a potassium atom on site 3 the charge transfer would be 65% (oxygen-chromium distance: 0.91 Å).

Our estimates are an upper limit of the charge transfer for a number of reasons. (a) The distance of the potassium to the oxygen atom is probably larger for an only partially ionized atom due to an increased atomic radius. (b) The strong relaxation within the first layers is very likely modified in the presence of an additional dipole layer on top of the surface. (c) The number of atoms per unit cell might be different, for example, two instead of one with site 1 as well as site 3 being occupied, which would mean even a halving of the dipole moment and the estimated charge transfer. The result of an incomplete charge transfer from the potassium atom to the chromium ions is consistent with our XPS data.

At coverages above $0.2\theta_{sat}$, the gradient of the work function decreases smoothly and finally drops to zero at θ_{sat} reflecting the conversion of potassium atoms from ionic to neutral with increasing coverage. The very shallow minimum around $(0.5\pm0.1)\theta_{sat}$ and the related small depolarization from a closer packing of the dipoles may be attributed to the relative large distance of Cr sites (site 1) of 5 Å for full packing and the rather localized character of the Cr $3d$ band.

5. XPS: Metal aggregate formation

By deposition of potassium at 90 K, any film thickness can be grown. Figure 6 shows the K $2p$ XP spectra for increasing coverages of potassium on $Cr_2O_3(0001)$. The gray shaded Voigt profile simulations have been obtained by fixing the maximum of the fitted $2p_{3/2}$ signal to the maximum of the experimental curve and assuming the fixed ratio of the $2p_{3/2}$ and $2p_{1/2}$ signal integrals of 2:1.

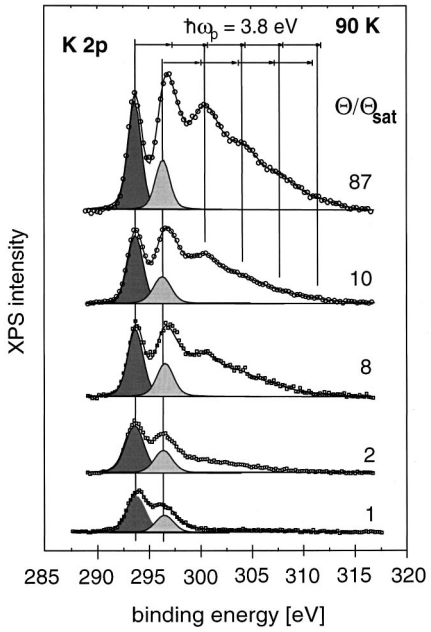

FIG. 6. Metal aggregate phase of potassium on $Cr_2O_3(0001)$: (a) Dotted curve: XP spectra of the K $2p$ emission as a function of increasing potassium coverage deposited with a low deposition rate at 90 K on $Cr_2O_3(0001)$; gray curves: fits assuming two Voigt profiles with maxima of $2p_{3/2}$ and $2p_{1/2}$ having a ratio of the integrals of 2:1 reflecting the multiplicity of the two states of 4:2; coverages are given as multiples of a maximal saturation coverage θ_{sat} at room temperature obtained from the integrals of K $2p$ XP spectra; detection geometry: 30° off normal emission.

The gradual evolution of additional intensity is observed at increasing coverages of potassium on the higher-binding energy side of the K $2p$ signal finally resulting in a long tailing of the spectrum with distinct new broad maxima at high coverages. The spacing of these new peaks is 3.8 eV corresponding to the plasmon energy of bulk potassium.[46] The surface plasmon of the flat potassium vacuum interface would be at 2.7 eV (i.e., a factor of $\sqrt{2}$ smaller) (Ref. 47), which is rather close to the spacing of the spin-orbit splitting of the K $2p$ signal. The resolution of our spectrometer is also too small to resolve the two peaks belonging to the $2p_{1/2}$ emission and the first bulk plasmon. The occurrence of plasmon excitations is indicative for the metallic character of the potassium aggregates. In view of the relatively low sensitivity of the method, the number of aggregates has to be substantial for plasmonic features to appear. Extra intensity such as in the lowest trace of Fig. 6 can show up as early as 10% of the saturation coverage. The occurrence of metal aggregates at a certain subsaturation coverage is influenced by the deposition rate used. This indicates a hit and sticklike growth at 90 K.

The work-function changes at low coverages for a deposition at 90 K are very similar to Fig. 5 though showing larger error bars as the data are more ambiguous with respect to the analysis of the XPS intensities. As there is no information about the growth mode of the aggregates other than the plasmon structure in XPS, the analysis of the potassium concentration from XPS data is only correct, if potassium grows in two-dimensional islands. Otherwise, the coverage

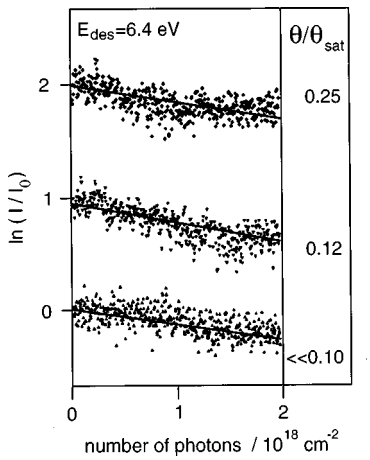

FIG. 7. Dispersive potassium phase on phase $Cr_2O_3(0001)$: Logarithmic plot of the depletion curves for different coverages of potassium dosed at room temperature measured for desorbing potassium in the gas phase as a function of photons impinged on the surface ($E_{des}=6.4$ eV); coverages are given as multiples of a saturation coverage θ_{sat} at room temperature obtained from the integrals of K $2p$ XP spectra.

of potassium is underestimated and the work-function curve would be more shallow than for the room-temperature case.

B. Laser-induced desorption of potassium from $Cr_2O_3(0001)$

1. Desorption cross sections

In order to determine the desorption efficiency of the laser-induced desorption of potassium from $Cr_2O_3(0001)$, the oxide surface was covered with a defined initial potassium coverage characterized by XPS and work-function measurements. The signal of desorbing neutral potassium atoms was measured as a function of the number of photons impinging on the surface. The available flux range was limited by the laser power and restrictions to the measurement time to avoid surface contaminations. No desorption of potassium ions was observed.

Desorption from the nonmetallic phase. Desorption of potassium atoms from the nonmetallic adsorbate state is mainly independent of the coverage. Figure 7 shows a plot of the logarithm of the desorption signal from the nonmetallic adsorbate state for three different coverages against the number of photons impinging on the surface. The two upper traces result from potassium coverages within the linearly decreasing part of the work-function curve. The lowest trace is recorded for a coverage of approximately $10^{-5}-10^{-4}$ of a monolayer as estimated from the REMPI intensities. Such a low coverage was obtained from potassium segregated after heating the oxide film and resulting from minute impurities of the Cr(110) crystal.

Assuming a desorption kinetics of first order, the curves in Fig. 7 may be approximated by straight lines. From the slope photodesorption cross sections of $(2\pm1)\times10^{-20}\,\mathrm{cm}^2$ are extracted for desorption energies of 3.5 eV and 5.0 eV and $(2\pm1)\times10^{-19}\,\mathrm{cm}^2$ for 6.4 eV, respectively.

The cross section at 6.4 eV is an order of magnitude larger than cross sections for the desorption from the ionic phase of potassium on graphite for which a maximum of $\leqslant(1.8\pm0.4)\times10^{-20}\,\mathrm{cm}^2$ was observed for an excitation energy of ~4.9 eV close to the interband transition at 4.8 eV of graphite.[21–23]

Desorption from potassium aggregates. The desorption efficiency from aggregates differs strongly with respect to the nonmetallic phase. We shall discuss three different cases for an excitation energy of 6.4 eV. The first paragraph deals with desorption from an adsorbate preparation in which the dispersed nonmetallic and a phase of medium-sized aggregates are simultaneously present. The second will discuss desorption from small 2D potassium aggregates and the third paragraph from large 3D aggregates. The data are representative for a larger number of measurements.

The preparation of a coverage with coexisting isolated nonmetallic atoms and potassium aggregates of medium size was realized by first depositing a saturation coverage at room temperature and then increasing the coverage at liquid-nitrogen temperature until first plasmonic structures appear within the K $2p$ spectrum (gray curves: fits assuming two Voigt profiles with maxima of $2p_{3/2}$ and $2p_{1/2}$ having a ratio of the integrals of 2:1). Two cross sections can be fitted to the resulting depletion curve [Fig. 8(a), left], a desorption cross section of $2.5\times10^{-19}\,\mathrm{cm}^2$ (similar to the nonmetallic phase of potassium) for the first several thousand laser pulses (1 mJ/cm^2), and a cross section an order of magnitude smaller ($3\times10^{-20}\,\mathrm{cm}^2$) for the second part. The overall intensity of the K $2p$ spectrum decreased substantially after this treatment [Fig. 8(a), right]. We interpret the first cross section as being due to desorption from the dispersive nonmetallic phase, and the second cross section due to the less efficient desorption from aggregates. A similar discontinuous drop in desorption efficiency has been reported for sodium desorption from sapphire when cooling the probe to 70 K, which was attributed to a phase transition between the 2D gas of adatoms to islet film formation.[14]

In a second preparation, the crystal was held at room temperature. Potassium was deposited with a high deposition rate to form a metastable coverage with plasmonic features in the XP spectra.[48] This preparation differs from the first one as the plasmonic structure lacks a pronounced tailing indicative for two-dimensional growth (gray curves: fits assuming two Voigt profiles with maxima of $2p_{3/2}$ and $2p_{1/2}$ having a ratio of the integrals of 2:1). As generally the island size has to surpass a critical size for 3D growth to occur in metal cluster growth,[25] the islands are likely to be small. The photodesorption signal of this preparation [Fig. 8(b), left] shows first an increase and then a decrease after a flat maximum. The decreasing part of the depletion curve takes a form typical for desorption of the nonmetallic species with a characteristic cross section of $2.5\times10^{-19}\,\mathrm{cm}^2$. The plasmonic structure is substantially reduced as seen in Fig. 8(b) right.

In a third preparation, potassium was deposited until the XP spectrum shows pronounced plasmonic features. For such large aggregates, a monotonic increase of the depletion signal is observed [Fig. 8(c), left]. At more than 8000 laser pulses (1 mJ/cm^2) the signal slowly approaches a saturation value while the integral of the K $2p$ signal in the XP spectra, still showing pronounced plasmonic structures, is decreased by 75% [Fig. 8(c) right].

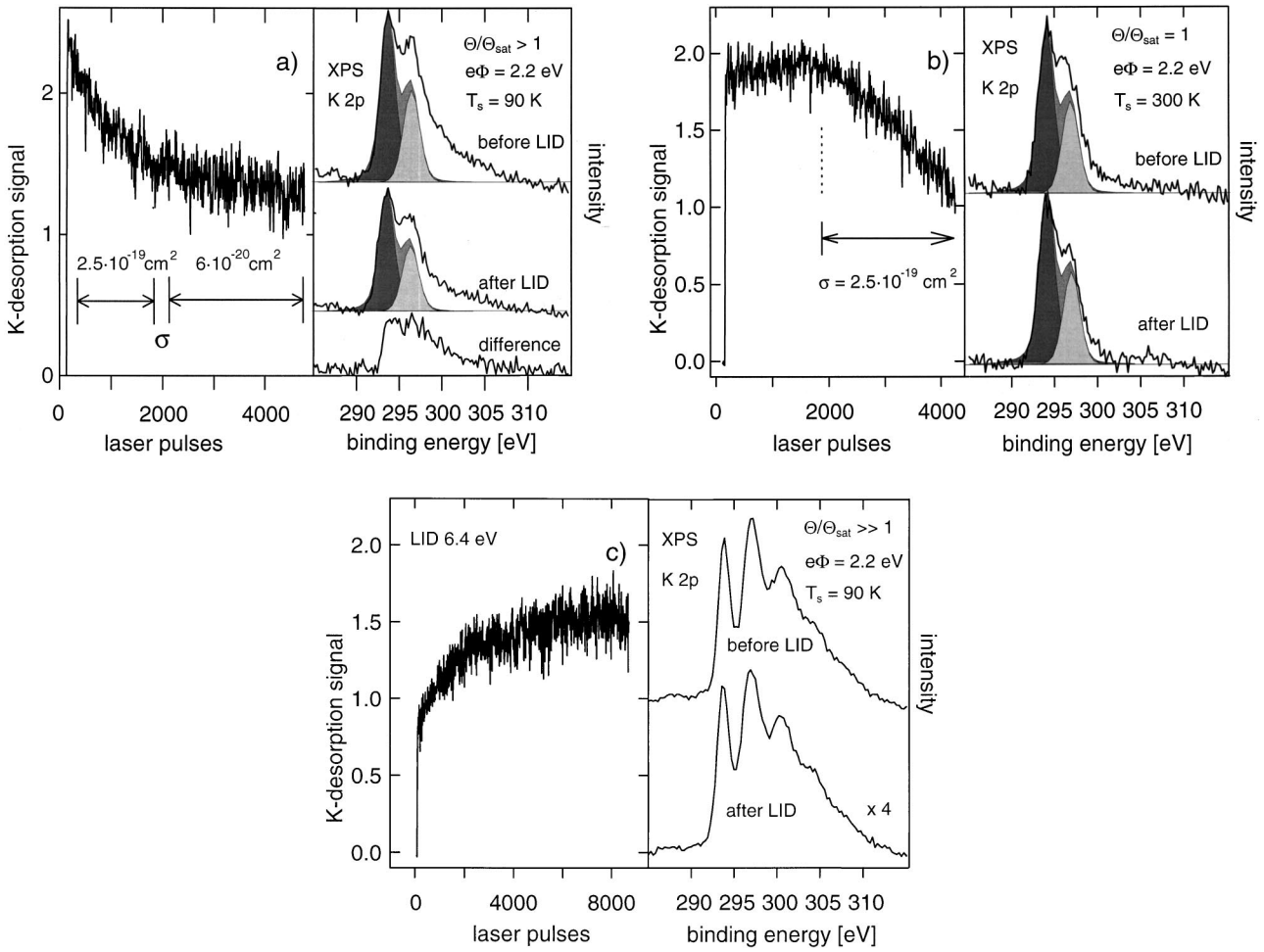

FIG. 8. Metal aggregate phase of potassium on Cr_2O_3(0001): gray curves: fits assuming two Voigt profiles with maxima of K $2p_{3/2}$ and K $2p_{1/2}$ (ratio of the integrals of 2:1 reflecting the multiplicity of the two states of 4:2). (a) Left: depletion curve of potassium dosed first at room temperature with a low deposition rate up to a maximal saturation coverage and then short dosing at 90 K; depletion measured for desorbing potassium in the gas phase as a function of photons impinged on the surface ($E_{\mathrm{des}}=6.4$ eV); the curve was fitted with two exponentials giving cross sections σ of 2.5×10^{-19} cm^2 and 3×10^{-20} cm^2. Right: XP spectra of the K $2p$ emission before (upper trace) and after (middle trace) registration of the depletion curve; lower trace: difference spectrum. (b) Left: depletion curve of potassium dosed at room temperature with a high deposition rate; depletion measured for desorbing potassium in the gas phase as a function of photons impinged on the surface ($E_{\mathrm{des}}=6.4$ eV); the second part of the curve was fitted with one exponential giving a cross section σ of 2.5×10^{-19} cm^2. Right: XP spectra of the K $2p$ emission before (upper trace) and after (lower trace) registration of the depletion curve. (c) Left: depletion curve of potassium dosed at 90 K (high coverage); depletion measured for desorbing potassium in the gas phase as a function of photons impinged on the surface ($E_{\mathrm{des}}=6.4$ eV). Right: XP spectra of the K $2p$ emission before (upper trace) and after (lower trace) registration of the depletion curve.

2. Velocity distributions

Time-of-flight distributions were recorded for a defined initial coverage characterized with XPS for three different desorption energies (3.5 eV, 5.0 eV, and 6.4 eV) and then transformed into velocity distributions. The data presented further below are all taken at 6.4 eV. The results are essentially the same for the two other desorption energies. No redosing was necessary during the experiment. Even for the most efficient process, as little as 0.03% of the overall coverage of potassium is desorbed per laser pulse at the laser fluences used. Therefore, the surface concentration can be treated as quasi-isoster on the time scale required for recording a velocity distribution in contrast to efficiency measurements.

Desorption from the nonmetallic phase. Figure 9(a) shows three different velocity distributions for a very small potassium coverage (10^{-5}–10^{-4} ML, obtained by segregation, see above) (lower trace), for a coverage around half of the saturation coverage (middle trace), and for a saturation coverage (upper trace) for adsorbates prepared by room-temperature deposition. The distributions were all normalized to the maximum intensity to make changes in shape visible. The maximum of the rather broad velocity distribution is found at 1800 m/s for the very low coverage corresponding to a most probable kinetic energy of 0.65 eV ($E_{\mathrm{kin}}/2k_B=3800$ K). The distribution cannot be fitted with one or two Boltzmann distributions. The full width at half maximum (FWHM) is 2600 m/s. For the adsorbate corresponding to the coverage at the work-function minimum [middle trace, Fig. 9(a)], a shift towards slower velocities is observed (1200 m/s). For the saturation coverage the maximum of the velocity distributions is further reduced to 1140

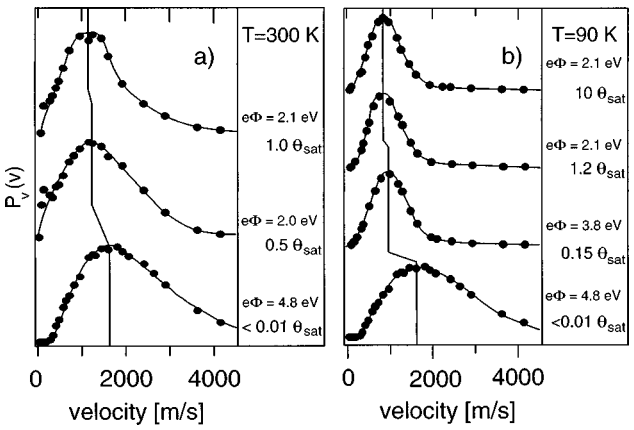

FIG. 9. Velocity distribution of desorbing potassium atoms: (a) Dispersive potassium phase on $Cr_2O_3(0001)$ (potassium dosed at room temperature; $E_{des}=6.4$ eV); lower trace: very small potassium coverage ($10^{-5}-10^{-4}$ ML); middle trace: $\Theta/\Theta_{sat}=0.5$; upper trace: $\Theta/\Theta_{sat}=1$. (b) Metal aggregate phase of potassium on $Cr_2O_3(0001)$ (potassium dosed at $T=90$ K; $E_{des}=6.4$ eV); first trace (from below): very small potassium coverage ($10^{-5}-10^{-4}$ ML) [as in (a)]; second trace: $\Theta/\Theta_{sat}=0.15$; third trace: $\Theta/\Theta_{sat}=1.2$; fourth trace: $\Theta/\Theta_{sat}=10$.

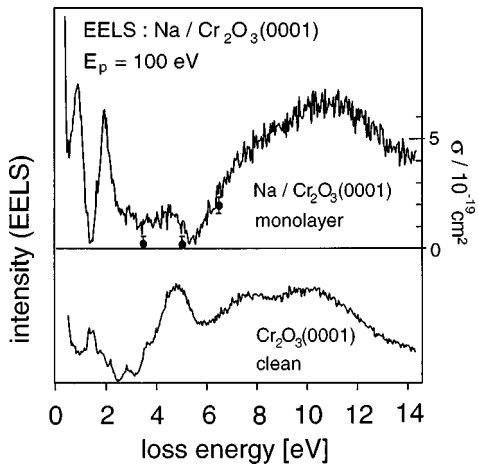

FIG. 10. Electron energy loss spectrum (EELS) of the clean $Cr_2O_3(0001)$ (lower trace) and a sodium-covered substrate (upper trace, submonolayer obtained by heating a multilayer to 520 K) taken from Ref. 34; $E_p=100$ eV, specular. Solid circles: desorption cross sections measured for the nonmetallic phase at $E_{des}=3.5$ eV, 5.0 eV, and 6.4 eV.

m/s corresponding to 0.26 eV ($E_{kin}/2k_B=1530$ K). This change is within the experimental accuracy of the velocity measurements of ± 100 m/s. However, the width of the velocity distribution is significantly reduced to a FWHM of 1500 m/s as compared to the middle curve with a FWHM of 2000 m/s.

Desorption from aggregates. The trend of decreasing velocities for increasing coverages continues when aggregate formation starts. Figure 9(b) shows three velocity distributions for potassium adsorbates deposited at 90 K exhibiting plasmonic structure in the XP spectra (three upper curves). The fourth distribution (lowest curve) is the velocity distribution of potassium traces already shown in Fig. 9(a) to make the overall change more distinct. The curve above the trace dosage corresponds to a coverage of 0.15 times the saturation coverage. For this aggregate the plasmonic features have disappeared after the recording of the velocity distribution. It is likely that the aggregates might be rather small in this case, and substantial changes of the overall structure might even occur on the time scale of this measurement. For a work-function change corresponding to bulk potassium, no further changes are visible when increasing the deposition as seen for the two upper curves. The desorbing atoms are rather slow with a velocity of 900 m/s at the maximum of the distribution, i.e., a kinetic energy of 0.16 ± 0.035 eV ($E_{kin}/2k_B=950$ K) and a FWHM of 1000 m/s as compared to the nonmetallic phase.

IV. DISCUSSION

To summarize, the following phenomena observed for laser-induced desorption of neutral potassium atoms from $Cr_2O_3(0001)$ have to be explained. (1) The desorption from the nonmetallic phase is ten times more efficient for isolated atoms than from metal aggregates and ranges from $\sigma=(2\pm1)\times10^{-19}$ cm^2 at an excitation energy of 6.4 eV to $\sigma=(2\pm1)\times10^{-20}$ cm^2 at 5.0 eV and 3.5 eV. (2) The desorption probability from metal aggregates increases with an increased amount of atoms desorbed from small aggregates of probably 2D structure as well as very large clusters of 3D structure. (3) The amount of desorbed species is substantial even for large aggregates. (4) The maxima of the velocity distributions shift with increasing coverage from 0.65 eV (isolated ionic species) to 0.16 eV (metal aggregates) while the FWHM of the velocity distributions decreases.

A. Inverse harpooning mechanism for desorption from the nonmetallic phase

As all excitation energies used are larger than the band gap of $Cr_2O_3(0001)$ in principle, two different nonthermal desorption processes are possible. Either states are directly excited within the adsorbate or an initial excitation occurs within the substrate followed by a subsequent intermediate charge transfer into an unoccupied state of the potassium.

Though the use of an excimer laser allows us to investigate desorption only at a restricted number of excitation energies, the data let us conclude that the excitation process for the nonmetallic phase is substrate induced as apparent from Fig. 10. The electron-energy-loss spectra (EELS) depicted are those of a pure and a sodium-covered $Cr_2O_3(0001)$ surface.[34] EELS data on potassium on $Cr_2O_3(0001)$ are not available, but potassium adsorption is rather similar to sodium. As is obvious from Fig. 10, the spectrum of the clean $Cr_2O_3(0001)$ surface is modified with alkali adsorption at energies around 4.6 eV related to a modification of surface charge-transfer transitions occurring from the O $2p$ band into a local Cr $3d$ state in this energy range.[34] In addition to this modification no resonant state can be attributed to alkali absorption in the energy range between 3.5 eV and 6.4 eV. The cross sections of the laser-induced desorption from the nonmetallic phase of potassium are plotted as a function of the excitation energy in Fig. 10 for comparison. It is obvious that the desorption cross sections mainly scale with the intensity of the excitation spectrum of the substrate.

The strong wavelength dependence of the desorption cross sections together with the high kinetic energies corresponding to more than 1000 K furthermore rule out a thermally induced process. The temperature jump within the epitaxial $Cr_2O_3(0001)$ film caused by laser heating is estimated to be only a couple of tens of K from solving heat flux equations[49] for a similar epitaxial film.[50]

The substrate-induced process can be regarded as an inverse harpooning mechanism.[51] A charge-transfer transition within the substrate is the primary excitation step followed by a migration of the electron to the surface. The hot electron is then trapped in an electronic state of the partially ionic potassium atom. The quasireneutralization is accompanied by a change of radius of the atom, which is known to be 137 pm for the isolated potassium K^+ ion and 203 pm for the neutral atom K^0.[36] As a consequence, the change of diameter causes a strong Pauli repulsion between the substrate and potassium. The potassium moves away from the surface until reaching a crossing between the two potential-energy surfaces of the ionic and neutral species in the adiabatic picture. The coupling between the two potential-energy surfaces is relevant for the branching between neutral potassium escaping from the surface and recapturing of the electron by the substrate with concomitant formation of ionic potassium. As only desorption from neutral potassium atoms is observed, the ion remains trapped. This excitation process has been discussed by Hellsing *et al.*[21,22] and Chakarov *et al.*[23] for desorption from ionic K adsorbed on graphite. Hellsing *et al.* pointed out that the described mechanism differs from the Menzel-Gomer-Redhead mechanism[52,53] in the sense that the repulsive state is not formed via primary excitation or ionization of the adsorbate-substrate complex itself by high-energy electrons or photons but corresponds to a two-step mechanism described by Gadzuk for photodesorption of NO from Pt(111).[54]

The decrease of translational excitation with increasing potassium coverage and the decrease of the FWHM of the velocity distribution can be attributed to the decreasing ionicity of potassium with increasing coverage that influences the position of the K $4s$ resonance state with respect to the Fermi edge. The minimum of the ground-state potential-energy surface with respect to the atom-surface distance shifts towards larger distances with decreasing ionicity. Starting from the potential-energy surface of a less ionic species, a more shallow part of the excited state is reached and thus less kinetic energy is gained.

It is known for TiO_2 that the electron density donated by the alkali atom to the substrate can partially penetrate deep into the space-charge layer at low coverages while at higher coverages it is localized to the surface dipole layer.[25] This might explain the strong difference between the velocity distribution of the segregation coverage and the larger coverages of potassium.

Surprising is the small dependence of the cross sections from the surface coverage of the ionic species compared to the strong changes in velocity distributions. Usually the cross sections are the most sensitive parameters with respect to changes within potential-energy surfaces.[52,53] Intuitively one expects an increasing lateral delocalization of excitation with an increasing number of dipoles at higher coverages and thus a related reduction of lifetime. This has been observed for other systems in electron stimulated desorption of molecules after valence-band excitation.[55] However, the effect is critically depending on the distance between the adsorbates. The minimum distance between two potassium atoms of 5 Å at full occupation of site 1 in the ionic phase is rather large, and the Cr $3d$ band is strongly localized. Furthermore, as discussed above, in case of alkali adsorption, the ionicity of the adsorbed atoms decreases with increasing coverage with a concomitant change of the potassium radius. Let us assume that the lifetime of the excited state is long enough so that the process can be described in an adiabatic picture as schematically shown in Fig. 11 for two different situations, i.e., the charge-transfer excitation of an ionic (a) and a less ionic species (b). The desorption probability then is ruled by the adiabatic coupling at the crossing point of the (in a first approximation) repulsive excited state of neutral potassium and the attractive ground-state potential of ionic potassium. The adiabatic coupling is depending on the difference in slopes between the two potential-energy surfaces and the velocity of the wave packet at the crossing point according to the Landau-Zener theory.[56] In case (a) the curve crossing occurs at a more shallow part of the potential-energy surfaces involved than for case (b). A decrease in slope difference causes a larger curve crossing probability and thus a decreased desorption probability. On the other hand, the velocity of the wave packet at the crossing point in case (a) is larger than in case (b), which causes a reduced curve crossing probability and a reduced recapture probability. The two effects may cancel each other in such a way that the desorption cross section becomes independent of the ionicity of the potassium atom. This is the case for crossing points occurring at rather large distances of the potassium atom to the surface with respect to the equilibrium position in the ground state as illustrated in Fig. 11, which is not unusual for a harpooning mechanism. The discussion assumes that the excited state for the ionic and less ionic species is the same, which is not necessarily the case. The desorption cross section is furthermore proportional to the cross section of primary adsorbate excitation. At higher coverages with less ionic potassium, one would expect a reduced initial trapping probability of electrons of the adsorbate.[22] However, this ef-

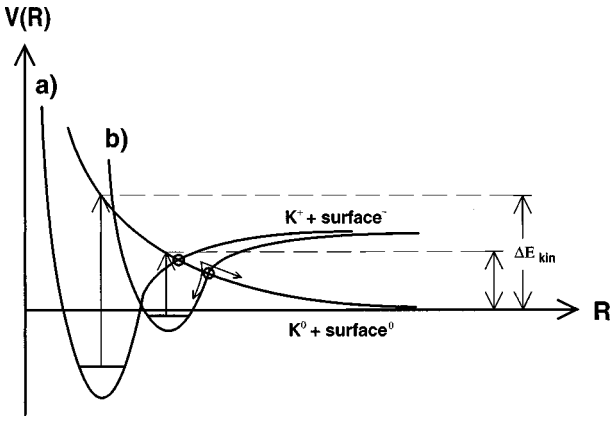

FIG. 11. Schematic drawing of the excitation process involving a charge-transfer transition in the adiabatic picture for (a) a strongly ionic atom and (b) a weakly ionic atom with a curve crossing occuring at large atom-surface distances (ΔE_{kin} is the gained kinetic energy after desorption).

fect is apparently also cancelled against the dependence of the cross section from the adiabatic coupling.

B. Localization of excition energy prior to desorption from metal aggregates

In the transition from the ionic phase to metallic islands, the closer contact of potassium atoms gradually changes the electronic structure of the adsorbate from discrete electronic states into a band structure with a delocalized gas of electrons for larger aggregates. As such an electronic structure allows an efficient quenching of electronically excited states, the drop of the cross sections by one order of magnitude has to be regarded as natural in this context. A similar argument holds for the drop of the most probable kinetic energy from 0.26 eV for the saturation coverage of the dispersive species (similar work function as metallic species) to 0.16 eV of the metal aggregates. The fact that we observe both, desorption from potassium aggregates and from the nonmetallic phase for the system $K/Cr_2O_3(0001)$, can be attributed to the higher laser flux when using an excimer laser compared to a mercury lamp used on graphite for which only desorption from the ionic phase was detected.[21–23]

As principally multiple excitation of plasmons within the metal aggregates is possible for the wavelengths used in our experiments, it is not clear whether the primary excitation process shifts from a substrate-mediated excitation process to a direct excitation within the metal aggregates. Initial plasmon excitation has been discussed to cause laser desorption for a variety of metal aggregates like potassium,[12] sodium,[8–16] and silver[12] on insulating supports. Similar processes are discussed for other metal atoms from metallic films of the same materials, e.g., for Al,[57] Au, and Ag atoms.[58,59]

The monotonic increase of the desorption signal with increasing depletion therefore may have two different causes. Either the number of desorption sites changes continuously or the increase is due to a continuous change of the electronic structure of the aggregates of diminishing size with concomitant changes of lifetimes of excited states and/or differences in absorbance as plasmon excitations are influenced by the size and shape of the aggregates[60–64] and dipole-dipole interactions among clusters (among other things).[65] We shall show that the first cause is apparently dominant implying localization of the primary excitation within local electronic states of defects as crucial for desorption.

If desorption from 2D islands took place preferentially from the interior of a perfect island, i.e., always from fully coordinated atoms, the desorption flux would decrease proportional to equivalent desorption sites available. Desorption purely from perfect edges would scale with the radius of the aggregates r, i.e., the signal would decrease. However, defect sites inside the clusters or dents of smooth cluster edges can act as nuclei for surface vacancy clusters. In this case the signal can grow with increasing radii of vacancy clusters. The preference of desorption from such sites can be explained by different local electronic properties as compared to regular terrace sites because of a reduced coordination number and has been observed in other experiments on atom desorption from metals, semiconductors, and insulator surfaces.[10,20,66–69]

The effect of increasing desorption signal with decreasing aggregate size will depend on the initial surface structure and thus on the growth conditions.[25] For amorphous aggregates or aggregates of dentridic shape, i.e., assemblies of high density of defect states, the increasing surface roughening would not be as pronounced as for initially mainly-ordered terraces. This could explain why a cross section was obtained for our first preparation for the metal aggregate component.

The observation of an increase in desorption signal for rather large clusters similar to 2D aggregates supports the explanation that defect desorption is the cause. The saturation of the desorption signal after long depletion of the large clusters then has to be regarded as reaching the maximal possible number of defect sites. The fact that the translational energy distributions of potassium desorbing from aggregates of metallic character are neither influenced by the excitation laser wavelength nor by the cluster size and related size-dependent plasmon resonances supports the interpretation of defect desorption.

In this context it is interesting to compare our data to experiments on potassium desorption from LiF(100).[12] Hoheisel, Vollmer, and Träger reported velocity distributions with a most probable kinetic energy of 0.13 ± 0.02 eV independent of the excitation wavelength covering the whole visible range with LiF(100) as support. This value is close to our data despite the fact that the data have been recorded under very different experimental conditions, i.e., with cw laser light for excitation energies below the band gap of the support and below bulk-plasmon excitation. We therefore conclude that either substrate-induced processes are of minor importance in this case or the primary excitation step is apparently mainly decoupled from the final desorption process. Furthermore, either the interaction of potassium with the support would be rather similar, if edge desorption were the cause, or the influence of the support on the electronic structure of defects would be small, in case defect desorption were the dominant channel.

While our data are surprisingly similar to the work on potassium clusters on LiF(100) (Ref. 12), strong deviations have been found for sodium desorption from a variety of different surfaces. Balzers *et al.* developed the picture that scattering of plasmons with surface vibrations causes desorption to explain their measured most probable kinetic energies of 0.018 ± 0.005 eV for desorption from sodium aggregates on mica.[13,15]

Träger and co-workers detected most probable kinetic energies of 0.4 ± 0.1 eV ($\lambda = 514$ nm) for sodium desorption from aggregates on LiF.[11,12] A value of 0.12 eV (700 K) was reported for the time-of-flight distribution of desorbing Na from a closed film of island structure with islands of 50–100 μm diam ($\lambda = 532$ nm) by Bonch-Bruevich *et al.*[18–20]) (the latter data were not taken under UHV conditions, and contaminations might have influenced the data).[18–20] Both groups discuss their data as being due to an initial plasmon excitation with a subsequent localization in defect states leading to desorption. The differences between the data of Balzers *et al.* and those of the other systems can be understood, if the interaction between the aggregate and the support plays a crucial role. Pinning of the electronic state responsible for desorption to the respective surface and rather different electron-lattice coupling for different supports could account for the discrepancies observed.

V. CONCLUSIONS

Potassium adsorbs on an epitaxial film of a Cr_2O_3(0001)/Cr(110) surface either in a nonmetallic phase at room temperature at Cr sites with a maximal saturation coverage at moderate deposition rates or as potassium aggregates at 90 K in any layer thickness desired. The interaction of single potassium atoms within the probably highly mobile nonmetallic phase is repulsive. At high deposition rates metastable aggregates are obtained at room temperature as these rates imply the formation of nucleation centers exceeding a critical size to stabilize the metallic aggregates. The work-function changes reflect a rather gradual change from ionic, with a partial charge transfer from potassium to chromium ions of maximally 55–65 % as upper limit, to neutral. The effect of depolarization at higher coverages is weak.

The initial excitation mechanism for the uv-laser-induced desorption of the ionic species is a charge transfer from the support to the potassium atom, which can be treated as inverse of a harpooning mechanism. A ten times more efficient desorption probability from the ionic species compared with metal aggregates reflects the localization of the temporal electronic excitation in the ionic species competing easily with electronic relaxation. On the other hand, efficient quenching of the electronically excited state within the metal aggregates necessitates localization in defect states or aggregate edges to enable desorption. The role of selvedges is evident from an increase of desorption probability with increasing photon exposure independent of the cluster shape and size. The properties of the selvedges of the metal aggregates rule the desorption process. This is apparent from the independence of the velocity distributions of the desorbing potassium atoms from the cluster size signifying a decoupling of the initial excitation from the final desorption process. On the other hand, the degree of interaction of the ionic species with the support is relevant for the amount of kinetic energy gained. This is revealed from a shift of the maxima of the velocity distributions with increasing coverage from 0.65 eV (isolated ionic species) to 0.26 eV (saturation coverage) to 0.16 eV (metal aggregates) and a concomitant decrease of the FWHM of the velocity distributions.

Theoretical calculations are planned to reveal details about the potential-energy surfaces of and lifetimes in the excited states of the ionic species as a function of ionicity. They should particularly help to clarify the origin of the weak coverage dependence of the cross section in contrast to the strong coverage dependence of the velocity distributions. Tentatively we attribute this observation to an electron recapture of the surface at large atom-surface distances, which is not unusual in harpooning processes.

Our results emphasize that aggregate size and structure, surface morphology as well as the interaction of the aggregate with the support, have to be carefully taken into account to explain and compare photodesorption data from alkaline adsorbates. If we regard the ionic dispersive potassium state as a ''single defect state'' with an elevated desorption probability compared to higher coordinated atoms, it would be very interesting to investigate other monodispersive systems with different adsorbate-substrate interactions and ionicities.

ACKNOWLEDGMENTS

The authors thank M. Bender for many helpful discussions on the adsorption behavior of alkali metals on oxide surfaces and H. Kuhlenbeck for useful suggestions. Thanks also go to Th. Klüner, V. Staemmler, D. R. Jennison, and H. Petek for discussions on the theory of alkali adsorption on oxides. The authors also thank Th. E. Madey and H. Petek for kindly sending them their manuscripts prior to publication.

*Present address: Institute of Industrial Science, The University of Tokyo, 7-22-1 Roppongi, Minato-ku, Tokyo 106-8558, Japan.
†Present address: Laser Zentrum Hannover, Hollerithallee 8, D-30419 Hannover, Germany.

[1] *Laser Spectroscopy and Photochemistry on Metal Surfaces*, edited by W. Ho and H.-L. Dai (World Scientific, Singapore, 1993).
[2] R. R. Cavanagh, D. S. King, J. C. Stephenson, and T. F. Heinz, J. Phys. Chem. **97**, 786 (1993).
[3] F. M. Zimmermann and W. Ho, Surf. Sci. Rep. **22**, 127 (1995).
[4] K. Al-Shamery, Appl. Phys. A: Mater. Sci. Process. **63**, 509 (1996).
[5] W. Ho, J. Phys. Chem. **100**, 13 050 (1996).
[6] S. Ogawa, H. Nagano, and H. Petek (unpublished).
[7] J. M. Chen and C. C. Chang, J. Appl. Phys. **43**, 3884 (1972).
[8] W. Hoheisel, K. Jungmann, M. Vollmer, R. Weidenauer, and F. Träger, Phys. Rev. Lett. **60**, 1649 (1988).
[9] W. Hoheisel, U. Schulte, M. Vollmer, R. Weidenauer, and F. Träger, Appl. Surf. Sci. **36**, 664 (1989).
[10] W. Hoheisel, U. Schulte, M. Vollmer, and F. Träger, Appl. Phys. A: Solids Surf. **51**, 271 (1990).
[11] W. Hoheisel, U. Schulte, M. Vollmer, and F. Träger, Z. Phys. D **20**, 381 (1991).
[12] W. Hoheisel, M. Vollmer, and F. Träger, Phys. Rev. B **48**, 17 463 (1993).
[13] F. Balzer, R. Gerlach, J. R. Manson, and H.-G. Rubahn, J. Chem. Phys.**106**, 7995 (1997).
[14] A. M. Bonch-Bruevich, T. A. Vartanyan, A. V. Gorlanov, and Yu. N. Maksimov, Zh. Eksp. Teor. Fiz. **97**, 1077 (1990) [Sov. Phys. JETP **70**, 604 (1990)].
[15] F. Balzer, M. Hartmann, M. Renger, and H.-G. Rubahn, Z. Phys. D **28**, 321 (1993).
[16] R. Gerlach, J. R. Manson, and H.-G. Rubahn, Opt. Lett. **21**, 1183 (1996).
[17] I. N. Abramova, E. B. Aleksandrov, A. M. Bonch-Bruevich, and V. V. Khromov, Pisma Zh. Eksp. Teor. Fiz. **39**, 172 (1984) [JETP Lett. **39**, 203 (1984)].
[18] A. M. Bonch-Bruevich, Y. N. Maksimov, S. G. Przhibel'skii, and V. V. Khromov, Zh. Eksp. Teor. Fiz. **92**, 285 (1987) [Sov. Phys. JETP **65**, 161 (1987)].
[19] A. M. Bonch-Bruevich, T. A. Vartanyan, Y. N. Maksimov, S. G. Przhibel'skii, and V. V. Khromov, Zh. Eksp. Teor. Fiz. **97**, 1761 (1990) [Sov. Phys. JETP **70**, 993 (1990)].
[20] A. M. Bonch-Bruevich, T. A. Vartanyan, Y. N. Maksimov, S. G. Przhibel'skii, and V. V. Khromov, Surf. Sci. **307-309**, 350 (1994).
[21] B. Hellsing and V. P. Zhdanov, J. Photochem. Photobiol., A **79**, 221 (1994).
[22] B. Hellsing, D. V. Chakarov, L. Österlund, V. P. Zhandov, and B.

Kasemo, J. Chem. Phys. **106**, 982 (1997).
[23] D. V. Chakarov, L. Österlund, B. Hellsing, V. P. Zhdanov, and B. Kasemo, Surf. Sci. Lett. **311**, L724 (1994).
[24] Th. E. Madey, B. V. Yakshinsky, V. N. Ageev, and R. E. Johnson, J. Geophys. Res. **103**, 5873 (1998).
[25] C. T. Cambell, Surf. Sci. Rep. **27**, 1 (1997).
[26] M. Wilde, I. Beauport, K. Al-Shamery, and H.-J. Freund, Surf. Sci. **390**, 186 (1997).
[27] M. Bender, K. Al-Shamery, and H.-J. Freund, Langmuir **10**, 3081 (1994).
[28] M. Bender, I. N. Yakovkin, and H.-J. Freund, Surf. Sci. **365**, 394 (1996).
[29] M. Menges, B. Baumeister, K. Al-Shamery, H.-J. Freund, C. Fischer, and P. Andresen, Surf. Sci. **316**, 103 (1994).
[30] S. Bashkin and J. O. Stoner, Jr., *Atomic Energy Level & Grotrian Diagrams 2, SulfurI-TitaniumXXII* (North-Holland, Amsterdam, 1978).
[31] The data are taken from Ref. 30. As the experimental data from Ref. 30 have been taken in air, the conversion from nm into cm^{-1} within the Grotrian diagrams of Ref. 30 takes into account the refractive index of air to account for different speeds of light in air and vacuum.
[32] K. Müller, G. Besold, and K. Heinz, in *Physics and Chemistry of Alkali Metal Adsorption*, edited by H. P. Bonzel, A. M. Bradshaw, and G. Ertl, Materials Science Monographs Vol. 57 (Elsevier, Amsterdam, 1989), p. 65.
[33] J. F. Moulder, W. F. Stickle, P. E. Sobol, and K. D. Bomben, in *Handbook of X-ray Photoelectron Spectroscopy*, edited by J. Chastain (Perkin Elmer Corporation, Prairie, MN, 1992).
[34] B. Dillmann, O. Seiferth, G. Klivenyi, F. Rohr, I. Hemmerich, M. Bender, I. Yakovkin, D. Ehrlich, and H.-J. Freund, Faraday Discuss. **105**, 295 (1996).
[35] M. Bender, Ph.D. thesis, Bochum, 1997.
[36] *CRC Handbook of Chemistry and Physics*, 78th ed., edited by D. R. Lide (Chemical Rubber, Boca Raton, FL, 1998).
[37] J. Hölzl and F. K. Schulte, in *Work-Function of Metals*, edited by G. Höhler, Springer Tracts in Modern Physics Vol. 85 (Springer, Berlin, 1979), p. 1.
[38] *Physics and Chemistry of Alkali Metal Adsorption* (Ref. 32).
[39] I. Langmuir, J. Am. Chem. Soc. **54**, 2798 (1932).
[40] R. W. Gurney, Phys. Rev. **47**, 479 (1935).
[41] C. Stampfl and M. Scheffler, Surf. Rev. Lett. **2**, 317 (1995).
[42] C. Su, X. Shi, D. Tang, D. Heskett, and K.-D. Tsuei, Phys. Rev. B **48**, 12 146 (1993).
[43] F. Rohr, M. Bäumer, H.-J. Freund, J. A. Meijas, V. Staemmler, S. Müller, L. Hammer, and K. Heinz, Surf. Sci. **372**, L291 (1997); **389**, 391E (1997).
[44] A. Leitheuser and V. Staemmler (private communication).
[45] K. Schäfer and C. Synowietz, *D'Ans-Lax Taschenbuch für Chemiker und Physiker, Bd. 3: Eigenschaften von Atomen und Molekülen* (Springer, Berlin, 1970).
[46] K. D. Tsuei and E. W. Plummer, Phys. Rev. Lett. **64**, 44 (1989).
[47] H. Raether, *Solid State Excitations by Electrons*, Springer Tracts in Modern Physics Vol. 38 (Springer, Berlin, 1972).
[48] By slightly heating such a preparation, the plasmonic features disappear.
[49] J. H. Bechtel, J. Appl. Phys. **46**, 1585 (1975).
[50] M. Menges, B. Baumeister, K. Al-Shamery, H.-J. Freund, C. Fischer, and P. Andresen, J. Chem. Phys. **101**, 3318 (1994).
[51] T. Greber, Surf. Sci. Rep. **28**, 1 (1997).
[52] D. Menzel and R. Gomer, J. Chem. Phys. **41**, 3311 (1964).
[53] P. A. Redhead, Can. J. Phys. **42**, 886 (1964).
[54] J. Gadzuk, Phys. Rev. B **44**, 13 466 (1991).
[55] D. Menzel, Nucl. Instrum. Methods Phys. Res. B **13**, 507 (1986).
[56] R. D. Levine and R. R. Bernstein, *Molecular Reaction Dynamics and Chemical Reactivity* (Oxford University Press, New York, 1987).
[57] I. Lee, J. E. Parks II, T. A. Callcott, and E. T. Arakawa, Phys. Rev. B **39**, 8012 (1989).
[58] I. Lee, J. E. Parks II, T. A. Callcott, and E. T. Arakawa, Phys. Rev. B **47**, 6661 (1993).
[59] M. J. Shea and R. N. Compton, Phys. Rev. B **47**, 9967 (1993).
[60] T. Götz, W. Hoheisel, M. Vollmer, and F. Träger, Z. Phys. D **33**, 133 (1995).
[61] J. H. Parks and S. A. McDonald, Phys. Rev. Lett. **62**, 2301 (1989).
[62] W. R. Holland and D. G. Hall, Phys. Rev. Lett. **52**, 1041 (1984).
[63] D. Steinmüller-Nethl, R. A. Höpfel, A. Leitner, F. R. Aussenegg, and A. Wokaun, Appl. Phys. A: Solids Surf. **57**, 261 (1993).
[64] P. Royer, J. L. Bijeon, J. P. Goudonnet, T. Inagaki, and E. T. Arkawa, Surf. Sci. **217**, 384 (1989).
[65] B. N. J. Persson and A. Liebsch, Phys. Rev. B **28**, 4247 (1983).
[66] K. Ishikawa, J. Kanasaki, Y. Nakai, and N. Itoh, Surf. Sci. **349**, L153 (1996).
[67] J. Viereck, F. Stietz, M. Stuke, T. Wenzel, and F. Träger, Surf. Sci. **383**, L749 (1997).
[68] M. A. Schildbach and A. V. Hamza, Phys. Rev. B **45**, 6197 (1992).
[69] M. Vollmer and F. Träger, Surf. Sci. **187**, 445 (1987).